The Kinetics of Substitution Reactions of Mixed Platinum(II) – Bis(nucleoside) Complexes in Aqueous Solution in the Presence of Thiourea; X-Ray Crystal Structure Determination of *cis*-$[Pt(NH_3)_2(adenosine\text{-}N7)_2](ClO_4)_2 \cdot 3.5\,H_2O$

Marjaana Mikola, Karel D. Klika, and Jorma Arpalahti*[a]

Abstract: In aqueous solution, bis(nucleoside) complexes formed by the reaction of *cis*-$[Pt(NH_3)_2(H_2O)_2]^{2+}$ with an excess of either adenosine (ado) or a mixture of adenosine and guanosine (guo) undergo a slow N7 → N1 linkage isomerisation in the adenine moiety. The isomerisation probably involves the breaking and reformation of Pt–nucleoside bonds, thus favouring the more stable N1 binding mode of the adenine base. Dynamic processes due to the presence of adenosine in the platinum coordination sphere are slow on the NMR time scale. The N7 binding mode of Pt^{II} in *cis*-$[Pt(NH_3)_2(ado\text{-}N7)_2](ClO_4)_2 \cdot 3.5\,H_2O$ was confirmed by X-ray crystal structure analysis. In both of the crystallographically independent cations, the Pt^{II} coordination sphere is almost ideally square planar, with typical Pt–N bond lengths and angles. The most significant difference between the two cations lies in the sugar conformation of the coordinated nucleosides. In one cation, both have an *anti* (*−ap*) conformation, whilst in the other cation one has an *anti* (*−ap*) conformation and the other a *syn* (*+sc*) conformation stabilised by a relatively strong H-bond. Substitution of the nucleoside(s) by thiourea follows an associative mechanism with only a negligible contribution by the solvent path. For symmetric complexes, the order of lability of different binding modes is ado-N1 < guo-N7 < ado-N7 for substitution of the first nucleoside, whereas for the second nucleoside it is guo-N7 < ado-N1 < ado-N7. For asymmetric complexes, the concomitant cleavage of different Pt^{II}–nucleoside bonds can be explained by two parallel reaction pathways. The change in the Pt^{II} coordination sphere affects the lability of the coordinating nucleosides in a different manner. The ado-N1 binding mode renders all binding modes less labile, whereas the ado-N7 mode has the opposite effect, and the guo-N7 mode increases the lability of the ado-N1 mode but decreases that of the ado-N7 mode. The mixed-ligand complex with (ado-N7)(guo-N7) mode is far more susceptible to attack by thiourea than the symmetric $(guo\text{-}N7)_2$ species. These two species can be considered as models for the two most abundant Cisplatin – DNA adducts.

Keywords: isomerizations · nucleobases · platinum · reaction mechanisms · substitution kinetics

Introduction

Interactions of Pt^{II} with the base residues in DNA are considered relevant to the biological activity of various anticancer Pt drugs.[1] The preponderant formation of intrastrand cross-links involving the guanine and adenine N7 sites is believed to play a key role in the action of Cisplatin (*cis*-$[PtCl_2(NH_3)_2]$) and related compounds.[1, 2] However, other binding modes cannot be completely ruled out, especially in the case of novel Pt drugs with *trans* geometry.[1, 2c, 3]

It is widely accepted that, once formed, the Pt – nucleobase complexes are inert under mild conditions and in the absence of strongly *trans*-labilising ligands.[4] In contrast, the presence of strong nucleophiles (e.g. sulfur-containing (bio)molecules, CN^-) facilitates the dissociation of N-bound nucleobases from the Pt coordination sphere. In particular, various sulfur-containing (bio)molecules have aroused considerable interest owing to their important roles in the biological processing of anticancer platinum drugs.[2b] Yet surprisingly little is known about the factors that affect the substitution reactions of Pt – nucleobase complexes, bearing in mind that not all platinum

[a] Dr. J. Arpalahti, M. Mikola, Dr. K. D. Klika
Department of Chemistry, University of Turku
20014 Turku (Finland)
Fax: (+358) 2-333-6700
E-mail: jorma.arpalahti@utu.fi

Supporting information (experimental details for NMR measurements; spectral data for the mixed Pt^{II} – bis(nucleoside) complexes: Table S1 for the ^1H chemical shifts, Table S2 for the ^{13}C and ^{195}Pt chemical shifts; observed rate constants for the dissociation of various bis-complexes in the presence of thiourea at different temperatures: Tables S3 – S5) for this article is available on the WWW under http://www.wiley-vch.de/home/chemistry or from the author.

0947-6539/00/0618-3404 $ 17.50+.50/0

bound to DNA can be removed with CN^- treatment.[5] The rate of displacement of guanosine from *cis*-$[Pt(NH_3)_2(guo\text{-}N7)_2]^{2+}$ by thiourea and other sulfur-containing nucleophiles, as well as by CN^-, has been studied by ^{13}C NMR spectroscopy.[6] A study of the reactions of *cis*- and *trans*-$[Pt(NH_3)_2(5'\text{-}GMP)_2]^{2-}$ (5′-GMP = 5′-guanosine monophosphate) in the presence of thiourea by HPLC has prompted the suggestion that the Pt–nucleobase bond is more labile than the Pt–NH_3 bond.[7] Substitution reactions of the 1:1 and 1:2 complexes of *cis*-$Pt^{II}(NH_3)_2$ with 1-methyluracilato anion have shown that the bis(methyluracilato) complex is inert to substitution by thiourea and I^-, unless the exocyclic O(4) atom is protonated.[8] The inertness of the bis(methyluracilato) complex parallels the behaviour of N3-platinated thymine and uracil complexes in the presence of CN^-, which has been attributed to the remarkable protective effect of the exocyclic oxygens.[9, 10] In Pt^{II}–bis(9-ethylguanine) complexes, orientation of the bases seems to affect the substitution reaction with CN^-, as demonstrated by the resistance of the head-to-tail complex compared with the head-to-head species.[10]

Nitrogen can also act as a nucleophile towards Pt^{II}, as demonstrated in a few cases by Pt–N bond rearrangements in both single-stranded and double-stranded oligonucleotides.[2c, 4, 11] The mechanisms of these bond rearrangements are not well understood; they may even require the cooperation of other nucleophiles such as Cl^-.[12] In model compounds, the intramolecular migration of coordinated Pt^{II} from endocyclic to exocyclic nitrogen has been observed in 1-methylcytosine[13] and in 9-methyladenine,[14] though in the former via Pt^{IV}. In fact, nitrogen has even been observed to displace sulfur-bound ligands from the Pt^{II} coordination sphere.[15]

Very recently, we have shown that the substitution reactions of monofunctional $[Pt(dien)(L\text{-}N7)]^{2+}$ (dien = diethylenetriamine, L = adenosine or guanosine) with thiourea in acidic aqueous solution follow a two-path nucleophile-dependent mechanism via pseudorotation of the pentacoordinate intermediate.[16] In this work we have studied the substitution reactions of various mixed-nucleoside complexes of *cis*-$Pt^{II}(NH_3)_2$ (Scheme 1) in aqueous solution by thiourea

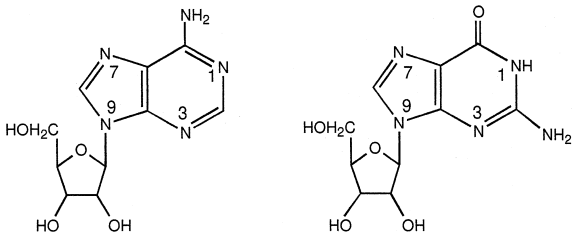

Binding modes with *cis*-$Pt^{II}(NH_3)_2$:

(ado-N7)$_2$ (**1**)	(guo-N7)$_2$ (**4**)
(ado-N1)(ado-N7) (**2**)	(ado-N1)(guo-N7) (**5**)
(ado-N1)$_2$ (**3**)	(ado-N7)(guo-N7) (**6**)

Scheme 1. The nucleoside complexes of *cis*-$Pt^{II}(NH_3)_2$ with adenosine and guanosine.

(pH 4) at different temperatures using HPLC as an analytical tool. The coordination sphere and binding modes of the nucleoside complexes were confirmed by ^{195}Pt and ^1H NMR spectroscopy, respectively. In addition, the X-ray crystal structure of *cis*-$[Pt(NH_3)_2(ado\text{-}N7)_2](ClO_4)_2 \cdot 3.5\,H_2O$ was determined.

Abstract in Finnish: *Vesiliuoksessa cis-$[Pt(NH_3)_2(H_2O)_2]^{2+}$-ioni muodostaa erilaisia 1:2 komplekseja adenosiinin (ado) tai adenosiinin ja guanosiinin (guo) kanssa, joilla havaitaan hidas Pt^{II}:n N7 → N1 sidoisomeraatio adeniinirenkaassa. Tämä johtunee adeniini-N1 sitoutumistavan suuremmasta termodynaamisesta pysyvyydestä verrattuna adeniini-N7 sitoutumiseen. Yhdisteen cis-$[Pt(NH_3)_2(ado\text{-}N7)_2](ClO_4)_2 \cdot 3.5\,H_2O$ kiderakenne määritettiin röntgendiffraktometrisesti. Alkeiskopissa on kaksi kristallograafisesti erilaista kationia, joissa platinan lähes tasoneliömäinen koordinaatiokehä on hyvin samanlainen. Merkittävin kationien välinen ero nähdään sokeriosan konformaatiossa (joko anti (−ap) tai syn (+sc); syn konformaatiota stabiloi vetysidos O(5′b) ⋯ N(3b) [2.74(2) Å]). Nukleosidien korvautuminen tiourealla noudattaa assosiatiivista mekanismia, jossa liuotintien osuus on vähäinen. Symmetrisillä komplekseilla sitoutumistavan labiilisuus noudattaa järjestystä ado-N1 < guo-N7 < ado-N7 tiourean korvatessa ensimmäisen nukleosidin. Toisen korvautuvan nukleosidin labiilisuus kasvaa sarjassa guo-N7 < ado-N1 < ado-N7. Epäsymmetrisillä komplekseilla kokonaisreaktio kulkee kahta reaktiotietä johtuen eri tavoin koordinoituneiden nukleosidien kilpailevasta korvautumisesta. Muutokset Pt^{II}:n koordinaatiokehällä vaikuttavat koordinoituneiden nukleosidien labiilisuuteen. Sitoumistavoista ado-N7 kasvattaa ja ado-N1 vähentää muiden sitoutumistapojen labiilisuutta. Sitoumistavalla guo-N7 on molemmat vaikutukset; ado-N1 muuttuu labiilimmaksi ja ado-N7 vähemmän labiiliksi.*

Results and Discussion

Isomerisation: Very recently we have shown that *cis*-$[Pt(NH_3)_2(9\text{-methyladenine})_2]^{2+}$ complexes undergo a slow N7 → N1 linkage isomerisation at elevated temperatures.[17] A similar process also occurs in the bis(adenosine) complexes of *cis*-$Pt^{II}(NH_3)_2$, and in mixed bis-complexes of Pt with guanosine and adenosine; both processes can be conveniently followed by HPLC (Figure 1). Under the chromatographic conditions employed,[18] all bis-complexes have longer retention times than the uncomplexed nucleosides. With bis(adenosine) complexes, the elution order **3** < **2** < **1** is the exact opposite of that found for the corresponding 9-methyladenine complexes.[17] In the preparation of mixed-ligand complexes, an excess of adenosine in the reaction mixture was employed to shift the product distribution towards **5** and **6**. This also caused the formation of traces of bis(adenosine) complexes and the different complexes followed the order of elution **4** < (**3**) < **5** < (**2**) < (**1**) < **6**. In both mixtures, the N7 coordination mode predominates at the beginning of the reaction, but the amount of the adenosine-N1-bound species slowly increases at the expense of the N7-bound species (Figure 2); this finding

  0947-6539/00/0618-3405 $ 17.50+.50/0

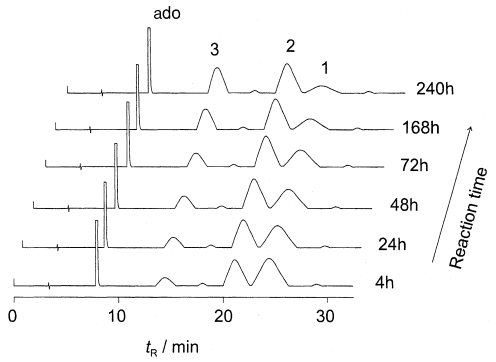

Figure 1. HPLC traces of the mixture of *cis*-$[Pt(NH_3)_2(H_2O)_2]^{2+}$ and adenosine at 60–70 °C at selected time intervals. Notation of complexes as Pt binding sites: 1: N7,N7; 2: N1,N7; 3: N1,N1.[18]

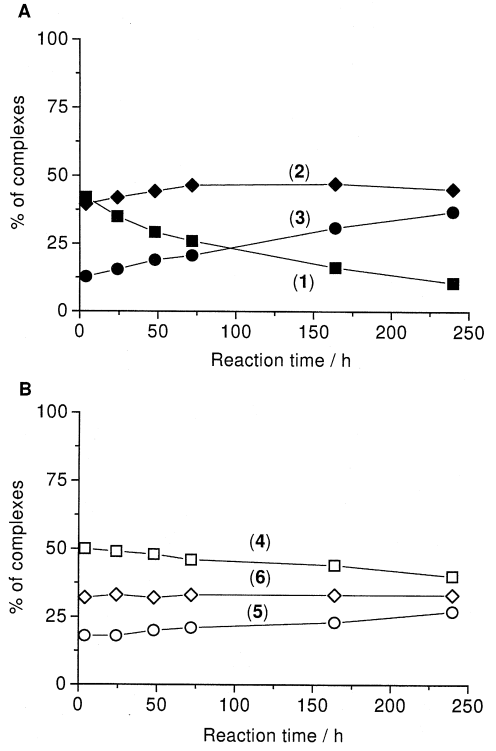

Figure 2. Results of isomerisation reactions of different Pt–nucleoside mixtures. A: Pt:ado = 1:2.4; B: Pt:guo:ado = 1:0.9:1.6 (the formation of traces of bis(adenosine) complexes is ignored).

is analogous to earlier results for *cis*-$Pt^{II}(NH_3)_2$ with 9-methyladenine,[17] and for Pt^{II}(dien) with adenosine[19] or 9-methyladenine.[20] However, under these conditions the N7 → N1 isomerisation occurs only in the adenine moiety. This is also expected by taking into account the high affinity of Pt^{II} for the N7 site in neutral guanine (Pt^{II} coordination to the guanine N1 site requires deprotonation of N1H).[21, 22] The high affinity of Pt^{II} for the guanine N7 site also accounts for the preponderance of **4** in the mixed-ligand system and the less efficient isomerisation compared with that of the adenosine system. Clearly, the isomerisation of **4** into mixed-ligand complexes **5** and **6** indicates the breaking and reformation of Pt–nucleobase bonds, although the data do not allow definitive conclusion about the reaction path (solvent-assisted or direct substitution) since both are expected to be slow.[16]

NMR studies: Table 1 lists the ^1H spectral data for **1**–**6** in the aromatic region; the complete spectral data are given in Table S1 for the ^1H chemical shifts and in Table S2 for the ^{13}C and ^{195}Pt chemical shifts (Supporting Information). In all complexes, the ^{195}Pt signal(s) appeared within the range of $\delta = -2500 \pm 100$, consistent with a PtN_4 coordination sphere.[23] The complexes all yielded a single platinum resonance, except for **3** which displayed two signals, belying the complexity generally seen in the ^1H and ^{13}C spectra where there was clear evidence of dynamic processes to various degrees as indicated by the splitting and/or broadening of the signals, sometimes to chaotic extremes. However, the ^{195}Pt signal-peak widths were generally much broader (in the range 800–1350 Hz) than normally observed for platinum nucleobase complexes (typically 500–800 Hz at 11.35 T).[14, 16, 17, 19, 20] The complexity of the conformational systems of the compounds varied from simple (two conformers) to extreme (several conformers present), indicating that at least a few processes in the extreme case were slow on the NMR time scale.

In all likelihood, one of the principle dynamic processes in effect is the restricted rotation of the nucleobase(s) about the Pt–N bond resulting from the close spatial proximity of the Pt^{II} atom and the exocyclic amino group of the adenine moiety.[17, 19, 20] This spatial proximity is particularly close for

Table 1. ^1H chemical shifts of the Pt^{II}–bis(nucleoside) complexes **1**–**6** in the aromatic region.[a]

Compound	$\delta_{H2(ado)}$		$\delta_{H8(ado)}$		$\delta_{H8(guo)}$
1[b]	8.312	(8.292)	8.998	(8.764)[c]	
	8.305	(8.240)[c]	8.954	(8.628)	
2[d]	8.804	[8.826][e, f]	8.934	[8.844][g, f]	
	8.790	[8.639][e]	8.913	[8.695][g]	
	8.445	[8.260][g]	8.420	[8.040][e, f]	
	8.424	[8.224][g, f]	8.400	[8.010][e]	
3[h]	8.868	{8.883}[f]	8.363	{8.158}[f]	
	8.786	{8.797}	8.356	{8.153}	
	8.763		8.335		
	8.724		8.323		
4[i]					8.376
5[j]	8.817		8.492		8.522
	8.806		8.443		8.503
6[k]	8.258		9.076		8.178
	8.256		9.063		8.161
ado[l]	8.146		8.283		

[a] In ppm from DSS (= 0); spectra recorded in D_2O. [b] Two conformers in the ratio 3:2; signals of the major species are listed on the first line and signals of the minor species on the second line. Data in parentheses refer to *cis*-$[Pt(NH_3)_2$(9-methyladenine-N7)$_2]^{2+}$.[17] [c] Questionable. [d] Because of insufficient material and an abundance of conformers (several), only a tentative assignment of this compound is possible; the signals are not listed in any particular order with respect to the conformers. Data in brackets refer to *cis*-$[Pt(NH_3)_2$(9-methyladenine-N1)(9-methyladenine-N7)$]^{2+}$.[17] [e] For N1-bound 9-methyladenine. [f] Minor species. [g] For N7-bound 9-methyladenine. [h] Four main conformers observed (ca. 90% in total) in the approximate ratio of 2:2:1:1 together with several less common species; the signals are not listed in any particular order with respect to the conformers. Data in braces refer to *cis*-$[Pt(NH_3)_2$(9-methyladenine-N1)$_2]^{2+}$.[17] [i] Only one conformer observed at 298 K, but exchange-related broadening clearly in evidence upon lowering the temperature to 277 K. [j] Two conformers (1:1) observed. [k] Two major species predominate (1:1), with a multitude of smaller conformers; the signals are not listed in any particular order with respect to the conformers. [l] From ref. [19].

0947-6539/00/0618-3406 $ 17.50+.50/0 *Chem. Eur. J.* **2000**, *6*, No. 18

the N1-bound species, and consistent with this, **2** and **3** display the strongest effects and conversely **4** the weakest effects (dynamic exchange effects were in fact only evident for **4** upon lowering the temperature to 4 °C). Another possible slow conformational process could be the interconversion between *syn* and *anti* orientations of the sugar ring with respect to the nucleobase; this conformational equilibrium would also explain the noticeable differences in chemical shift for some of the sugar protons between the various conformers. Rotation about the C1′–N9 bond may be slow owing in part to steric hindrance and/or intramolecular hydrogen bonding between the sugar and the nucleobase, but certainly platinated nucleotides have been shown to be composed of an equilibrium mixture of *syn* and *anti* conformers in solution.[24]

For **1**, both *syn* and *anti* orientations were in fact observed in the solid state (see below). Two conformers (ratio 3:2) were observed in solution, and the major species was identified as *syn* on the basis of NOE and ROE difference experiments which showed discernible enhancements (2.8 %) at H1′ upon irradiation of H8, although the exchange process complicated the interpretation, particularly in the reverse direction. The lack of an NOE from H8 to H1′, together with the marked chemical shift difference of both H2′ and H3′ in the minor species of **1** compared with their counterparts in the major species, led to the assignment of the minor species as the *anti* conformer. Although another conformational process may be occurring together with the *syn*/*anti* equilibrium, and thus the *syn*/*anti* equilibrium need not necessarily be slow in this case (the two conformers representing instead a concomitant shift in the *syn*/*anti* equilibrium, since this exchange can be fast[24]), nevertheless it remains valid to describe the two conformers as *syn* and *anti*.

The two conformers of **1** also showed clear changes in the position of the north/south ring conformational equilibrium[24] of the sugar moiety (this conformational change is known to be fast on the NMR time scale[24, 25]) as evidenced by the magnitude of the proton vicinal coupling constants[25]—and indeed this is also expected to occur in concert with a *syn* and *anti* interconversion.[24] In contrast to expectations, though,[24] it is the *syn* conformer for which the north/south ring conformational equilibrium is more biased towards the north conformer (60 %, vs. 50 % for the *anti* conformer). This difference between the *syn* and *anti* conformers is also echoed in the crystal structure, where the *syn* and *anti* conformers possess different sugar-ring conformations.

The position of the north/south sugar-ring conformational equilibrium has been shown to be affected by the binding of platinum to the nucleobase,[24] and there are clear distinctions between the equilibrium position of the sugar-ring conformation and the different binding modes, but the equilibrium position is also heavily influenced by other factors such as conformational change (e.g. as in **1**), hydrogen bonding, anomeric effects, *gauche* effects etc.[24, 25] Other possible dynamic exchange equilibria could include dimerisation, either through intermolecular hydrogen bonding[26] or base stacking,[25, 26] though the former is unlikely given the polarity of the solvent used here, and although speculative, the latter would nevertheless show markedly concentration- and temperature-dependent spectra (which was indeed the case for some samples, e.g. **5**).

Nonetheless, the observed ^{1}H chemical shifts confirm the binding modes of Pt^{II} in the adenine moiety by showing significant downfield shifts for those signals near the proposed coordination site and by comparison with the data for the isomeric bis(9-methyladenine) complexes[17] of *cis*-$Pt^{II}(NH_3)_2$ and the Pt^{II}(dien) complexes of adenosine.[19] The ^{13}C chemical shifts are also consistent with the assigned structures (particularly with respect to the type of nucleobase), but seemingly do not provide such a reliable guide for full structural assignment.[14, 16, 17, 19, 20]

X-ray crystallography: The X-ray crystal structure analysis confirms the N7 binding mode of Pt^{II} in *cis*-$[Pt(NH_3)_2(ado\text{-}N7)_2](ClO_4)_2 \cdot 3.5\,H_2O$ (**1a**). One of the two crystallographically independent cations of **1a** is shown in Figure 3; the

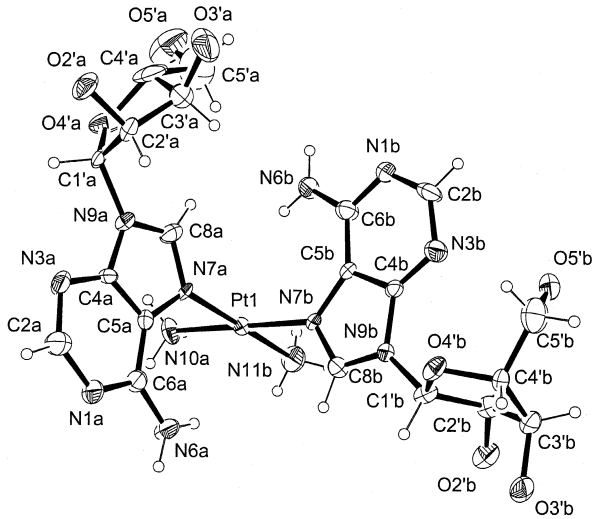

Figure 3. ORTEP[41] plot showing 30 % probability ellipsoids of one of the two crystallographically independent cations of **1a**, with atom-labelling scheme. Selected interatomic distances (Å) and angles (°) with estimated deviations in parentheses: Pt(1)–N(7A) 2.021(10), Pt(1)–N(7B) 2.046(10), Pt(1)–N(11B) 2.047(11), Pt(1)–N(10A) 2.052(11), N(7A)-Pt(1)-N(7B) 91.9(4), N(7A)-Pt(1)-N(11B) 177.2(5), N(7B)-Pt(1)-N(11B) 90.8(5), N(7A)-Pt(1)-N(10A) 87.4(4), N(7B)-Pt(1)-N(10A) 179.0(5), N(11B)-Pt(1)-N(10A) 89.9(5).

second cation is quite similar. In both cations, the Pt^{II} coordination sphere is almost square planar with normal Pt–N bond lengths and angles, and the complexed nucleobases are orientated in a head-to-tail fashion. The dihedral angle between the base moieties denoted as A and B is 83.3(3)°, and that between the base moieties denoted as C and D (cation not shown) is 86.3(3)°. The Pt^{II} atom lies virtually in the plane defined by the four coordinating nitrogen atoms and deviates by less than 0.01 Å from this plane in both cations. Notable differences between these two species can been seen in the sugar orientation. In the cation depicted in Figure 3, nucleoside A has an *anti* (*–ap*) conformation [torsion angle O(4′a)-C(1′a)-N(9a)-C(4a) –154(1)°], whilst nucleoside B has a *syn* (*+sc*) conformation [torsion angle O(4′b)-C(1′b)-N(9b)-C(4b) 52(2)°].[27] In the second cation, both coordinated adenosine moieties, C and D, have an *anti* (*–ap*)

conformation [torsion angles O(4′c)-C(1′c)-N(9c)-C(4c) $-165(1)^\circ$, and O(4′d)-C(1′d)-N(9d)-N(4d) $-157(1)^\circ$, respectively].

The packing of **1a** is stabilised by extensive hydrogen bonding involving the NH_3 or NH_2 hydrogens and perchlorate or water oxygens. The shortest nonbonded contacts include e.g. N(6a)-H(6a2)···O(34[a)]) 2.87(2) Å, N(6c)-H(6c2)···O(42[b)]) 2.87(2) Å, N(10a)-H(10a2)···O(4W) 2.92(2) Å, and N(11d)-H(11d3)···O(13a[c)]) 2.86(5) Å. The endocyclic nitrogens may also be participating in hydrogen bonding. Most notable is the relatively strong contact O(5′b)···N(3b) of 2.74(2) Å, which probably stabilises the *syn* conformation of nucleoside B. In addition, the exocyclic amino groups may form hydrogen bonds to the endocyclic N1 sites, specifically N(6a)-H(6a1)···N(1d[a)]) 2.97(2) Å, N(6b)-H(6b1)···N(1c[d)]) 3.10(2) Å and N(6c)-H(6c2)···N(1b[b)]) 3.10(2) Å. Further close contacts exist between the water molecules and sugar hydroxyl groups, for instance O(2W)···O(5W) 2.80(2) Å, O(2W)···O(3′a) 2.70(2) Å, O(3W)···O(5W) 2.50(3) Å, O(3W)···O(7W[e)]) 2.55(3) Å, O(3W)···O(2′a[f)]) 2.62(3) Å, O(6W)···O(5′b[e)]) 2.71(2) Å and O(7W)···O(2′b) 2.73(3) Å. [Symmetry operations: a) $-x+½, -y+1, z+½$; b) $-x-½, -y+1, z-½$; c) $x, y, z-1$; d) $-x-½, -y+1, z+½$; e) $-x, y+½, -z+½$; f) $x-½, -y+½, z$]. The stacking of the nucleobases, in contrast, seems to be unimportant in stabilising the lattice of **1a**, since the distances between the centres of the 6- and 5-membered rings of the neighbouring bases are >4.5 Å. The N(6)···Pt distances in **1a** range from 3.43(1) Å (unit D) to 3.55(1) Å (unit A), agreeing with the values reported for the corresponding complex of 9-methyladenine.[17]

Substitution reactions: On the basis of the HPLC analysis, we can say that all the complexes studied react with a similar overall mechanism. The action of thiourea (tu) resulted in the formation of free nucleoside(s) and $[Pt(tu)_4]^{2+}$ as the final products in all cases. For the homogeneous bis(nucleoside) complexes **1**–**4**, the HPLC analysis gave a ratio of 2:1 for the end products (nucleoside:$[Pt(tu)_4]^{2+}$); for the heterogeneous nucleoside complexes **5** and **6** the end-product ratio was 1:1:1 (adenosine:guanosine:$[Pt(tu)_4]^{2+}$), as quantified by authentic samples. In all cases, though, the nucleoside(s) began to accumulate earlier than $[Pt(tu)_4]^{2+}$, an observation suggestive of a stepwise substitution reaction. This mechanism is further supported by the fact that additional species were detected during all the substitution reactions (Figure 4). These were first formed and then consumed in the overall reaction, indicating a species capable of further reaction with thiourea. Thus the overall substitution seems to follow the pathway depicted in Scheme 2, assuming that the NH_3 group is more tightly bound to Pt^{II} than a nitrogen-coordinated nucleobase upon attack by the first thiourea molecule. This is a reasonable assumption given the high thermodynamic stability of the Pt^{II}–NH_3 bond.[28] Accordingly, after thiourea first displaces one nucleoside from the Pt coordination sphere, a rapid substitution of the NH_3 group *trans* to thiourea follows, which yields a UV-detectable intermediate(s) denoted as **IL** (or **IL1** and **IL2** for asymmetric species **2**, **5** and **6**, vide infra). The subsequent attack of thiourea on this intermediate liberates the second nucleoside followed again by the rapid displacement of the remaining NH_3 group yielding $[Pt(tu)_4]^{2+}$ as the final Pt species. In fact, this type of reaction pathway has already been proposed for the reaction of thiourea with *cis*-$[Pt(NH_3)_2(5'\text{-GMP})_2]^{2-}$.[7]

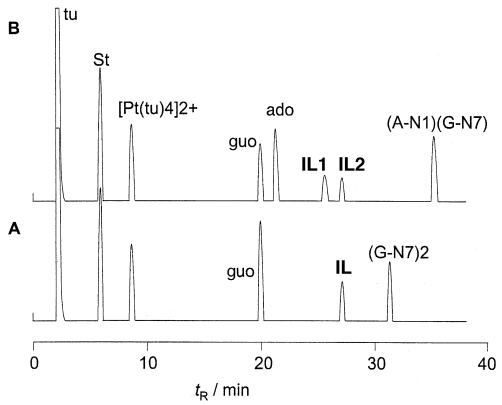

Figure 4. HPLC traces of the mixtures of thiourea with *cis*-$[Pt(NH_3)_2(guo\text{-}N7)_2]^{2+}$ (A) and *cis*-$[Pt(NH_3)_2(ado\text{-}N1)(guo\text{-}N7)]^{2+}$ (B) after one half-life. Notation of the intermediates: A: **IL**; B: **IL1** and **IL2** (= **IL**). Gradient elution with 0.05 M $NaClO_4$ (pH 3) as an eluent (3 → 15% methanol/15 → 26 min, 1.0 mL min^{-1}).

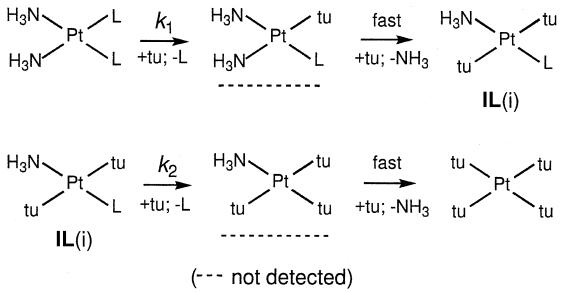

Scheme 2. Pathway of the thiourea substitution reaction for symmetric nucleoside complexes of *cis*-$Pt^{II}(NH_3)_2$.

Although the pathway depicted in Scheme 2 adequately describes the substitution reactions of the symmetric complexes **1**, **3** and **4**, a more complex mechanism is required for the asymmetric species **2** and the mixed nucleoside complexes **5** and **6**. According to chromatographic analysis, the complexes **2**, **5** and **6** all gave two different intermediates **IL1** and **IL2**, and in the cases of **5** and **6**, both nucleosides were already formed at the beginning of the reaction. These findings strongly suggest that the first rate-determining steps consist of two parallel pathways, as shown in Scheme 3. The retention times of the intermediates between relevant species lend further support to the proposed mechanism (Figure 4). For example, one of the two intermediates of **2** has practically the same retention time as the single intermediate of **3**, while the retention time of the other agrees with the single intermediate observed for **1**. Similar analogies were also seen between the intermediates of **5** and those of **3** and **4**, and for the intermediates of **6** and **1** and **4**.[29]

Pseudo-first-order rate constants, $k_{1,obs}$ and $k_{2,obs}$, at different temperatures are listed in Tables S3, S4 and S5 (Supporting Information). The values of $k_{1,obs}$ were obtained from the rate of disappearance of the starting material by Equation (3), and the values of $k_{2,obs}$ by Equation (4) (see Experimental

0947-6539/00/0618-3408 $ 17.50+.50/0 *Chem. Eur. J.* **2000**, *6*, No. 18

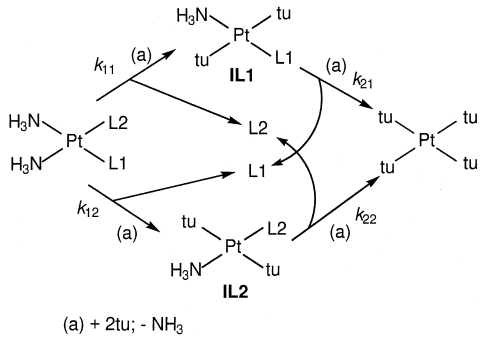

Scheme 3. Likely parallel pathways of the thiourea substitution reaction for asymmetric nucleoside complexes of *cis*-$Pt^{II}(NH_3)_2$.

Section) from the time-dependent concentration of the intermediate(s). In the case of **2**, **5** and **6**, the data for $k_{1,obs}$ refer to the sum of the individual rate parameters of the parallel steps, $k_{11,obs} + k_{12,obs}$. In each kinetic run the ratio $r = k_{11,obs}/k_{12,obs}$ was obtained by least-squares fitting to Equation (1) (see Scheme 3 for notation of the rate parameters). In

$$\frac{[\mathbf{IL\,1}]}{[\mathbf{IL\,2}]} = r\frac{[k_{1,obs} - k_{21,obs}][e^{-k_{1,obs}t} - e^{-k_{22,obs}t}]}{[k_{1,obs} - k_{22,obs}][e^{-k_{1,obs}t} - e^{-k_{21,obs}t}]} \quad (1)$$

the fitting procedure,[30] all rate parameters were fixed using the experimentally determined values, and the fitted values for the r term listed in Tables S3 – S5 were practically constant for different thiourea concentrations at any given temperature. The concentration ratio of the intermediates **IL 1** and **IL 2** on the left-hand side of Equation (1) was approximated from the HPLC traces by using the peak areas of these species at 260 nm, which is near the λ_{max} values for various purine nucleosides bearing Pt^{II} at the N1 or N7 site.[31, 32] In addition, the apparent ratios of different N1- and N7-bound Pt^{II} – adenosine 1:1 complexes do not differ significantly from the quantified ratios even when based on peak heights.[31] Hence, it seems safe to assume that the peak areas quantified at 260 nm do give a reliable approximation of the concentration of the different intermediates.

In the case of **6**, co-elution of the intermediates **IL 1** and **IL 2** hampered the determination of the individual rate constants $k_{11,obs}$ and $k_{12,obs}$ by Equation (1). Hence, these rate parameters were approximated from the time-dependent formation of the free nucleosides by means of Equation (2). Here the concentrations of the nucleosides L1 and L2 refer to normalised values using the final peak areas of these species. The data for $k_{11,obs}$ and $k_{12,obs}$ listed in Tables S3 – S5

$$\frac{[\mathbf{L\,1}]}{[\mathbf{L\,2}]} = \frac{(k_{22,obs} - k_{1,obs})[k_{21,obs} - k_{1,obs} - (k_{21,obs} - k_{12,obs})e^{-k_{1,obs}t} + k_{11,obs}e^{-k_{21,obs}t}]}{(k_{21,obs} - k_{1,obs})[k_{22,obs} - k_{1,obs} - (k_{22,obs} - k_{11,obs})e^{-k_{1,obs}t} + k_{12,obs}e^{-k_{22,obs}t}]} \quad (2)$$

for **6** were obtained by the use of fixed values for the parameters $k_{1,obs}$, $k_{21,obs}$ and $k_{22,obs}$ with experimentally determined values for $k_{1,obs}$, and data obtained from the symmetric species **1** and **4** for $k_{21,obs}$ and $k_{22,obs}$, respectively.[30] For comparison, the parameters $k_{21,obs}$ and $k_{22,obs}$ were also allowed to vary freely with only $k_{1,obs}$ fixed, yielding comparable values for all rate constants; the data are included in Tables S3 – S5. In order to check the reliability of the computations by Equation (2) the rate constants for **5** were treated in a similar manner. In each case the agreement between the values found for the rate constants $k_{11,obs}$, $k_{12,obs}$, $k_{21,obs}$ and $k_{22,obs}$ by Equations (1) and (2) was reasonable (Tables S3 – S5), supporting the validity of the data.

For symmetric species **1**, **3** and **4**, plots of $k_{i,obs}$ vs. [tu] gave the second-order rate parameters k_1 and k_2 for the rate-determining steps (Table 2). In the case of **2**, **5** and **6**, similar treatment was applicable for $k_{21,obs}$ and $k_{22,obs}$, whereas plots of $k_{1,obs}$ yielded only the sum of the rate constants of the parallel steps, which were transformed into individual parameters by the mean values of the ratios obtained by Equation (1) for **2** and **5**, and by Equation (2) for **6**; the data are included in Table 2. The small value, usually ca. $10^{-6}\,s^{-1}$ (occasionally a small negative value was obtained), for the intercept of the plot of $k_{i,obs}$ vs. [tu] indicates that the contribution of the solvent path is negligible in both rate-determining steps. The second-order rate constant for the replacement of one guanosine ligand in **4** with thiourea of $(5.9 \pm 0.6) \times 10^{-5}\,M^{-1}\,s^{-1}$ at 316 K, obtained by ^{13}C NMR, is in good agreement with our data.[6a] Upon dissociation of the first nucleoside, the reactivity of the bis-complexes follow the

Table 2. Second-order rate parameters, k_i [$10^{-5}\,M^{-1}\,s^{-1}$], for the rate-determining steps in the dissociation of **1** – **6** in aqueous solution (pH 3 – 4) in the presence of thiourea.[a]

Compound	T [K]	k_1[b]	k_{11}	k_{12}	k_2[c]	
1	318.2	22.8 ± 0.5			11.3 ± 0.03	
	328.2	65 ± 3			31.6 ± 0.06	
	338.2	163 ± 5			74.3 ± 0.06	
2	318.2	7.4 ± 0.2	4.3 ± 0.2[d]	3.1 ± 0.2[e]	7.0 ± 0.2[e]	12 ± 1[d]
	328.2	21.2 ± 0.1	12.4 ± 0.1[d]	8.8 ± 0.1[e]	18.5 ± 0.1[e]	34 ± 1[d]
	338.2	49 ± 2	29 ± 2[d]	20 ± 2[e]	47.6 ± 0.2[e]	82 ± 1[d]
3	318.2	2.16 ± 0.05			6.8 ± 0.1	
	328.2	6.3 ± 0.3			18.3 ± 0.3	
	338.2	19.1 ± 0.1			46.2 ± 0.3	
4	318.2	7.96 ± 0.05			3.70 ± 0.05	
	328.2	22.2 ± 0.5			9.6 ± 0.7	
	338.2	63.6 ± 0.9			23.2 ± 0.2	
5	318.2	5.93 ± 0.07	3.36 ± 0.07[f]	2.57 ± 0.07[e]	7.3 ± 0.6[e]	4.0 ± 0.1[f]
	328.2	15.2 ± 0.2	8.7 ± 0.2[f]	6.5 ± 0.2[e]	17.9 ± 0.1[e]	9.5 ± 0.2[f]
	338.2	39.1 ± 0.7	22.6 ± 0.7[f]	16.5 ± 0.7[e]	47 ± 2[e]	24 ± 1[f]
6	318.2	14.7 ± 0.5	10.1 ± 0.5[f]	4.6 ± 0.5[d]	12 ± 1[d]	4.6 ± 0.2[f]
	328.2	42 ± 2	29 ± 2[f]	13 ± 2[d]	35 ± 1[d]	12.6 ± 0.4[f]
	338.2	99.5 ± 0.4	70.0 ± 0.4[f]	29.5 ± 0.4[d]	79 ± 3[d]	28 ± 3[f]

[a] Data for k_i refer to the slopes of the plots $k_{i,obs}$ vs [tu]. [b] For asymmetric species **2**, **5** and **6**, the data refer to the sum constant $k_1 = k_{11} + k_{12}$, which gives the parameters for the parallel steps k_{11} and k_{12} from the mean value of the ratio $r = k_{11,obs}/k_{12,obs}$ at given temperature. [c] Includes the rate constants k_2, k_{21} and k_{22}. [d] For the cleavage of the ado-N7 bond. [e] For the cleavage of the ado-N1 bond. [f] For the cleavage of the guo-N7 bond.

order **3** < **5** < **2** ≈ **4** < **6** < **1**. When the statistical factor in the symmetric species is taken into account, the increased lability of the different binding modes in the first step follows the order ado-N1 (**3**) < ado-N1 (**5**) < ado-N1 (**2**) ≈ guo-N7 (**5**) < guo-N7 (**4**) ≈ ado-N7 (**2**) ≈ ado-N7 (**6**) < guo-N7 (**6**) ≈ ado-N7 (**1**) with relative rate constants of 1:2.4:2.9:3.1:3.7:4.0:4.3:9.4:10.6 at 318.2 K. This order also remains the same at higher temperatures, though the differences in reactivity become slightly smaller. Upon dissociation of the second nucleoside, however, the lability order of the binding modes changes to guo-N7 < ado-N1 < ado-N7 with relative rate constants of ca. 1:1.9:3.2 at all temperatures.

Activation parameters for the rate-determining steps are listed in Table 3. In all cases, the negative $\Delta S^{\neq}$ values suggest an associative mechanism for the substitution reactions, as is usual for Pt^{II}. The activation parameters for the symmetric species seem to differ from those for the asymmetric ones in the first rate-determining step. At least with **3** and **4**, the retarding effect of the large positive $\Delta H^{\neq}$ term is, however, cancelled by the more favourable $\Delta S^{\neq}$ term. In the second rate-determining step the activation parameters for the two binding modes of adenosine are very similar, differing from the guo-N7 mode by the more negative $\Delta S^{\neq}$ term of the latter. To some extent the data found for the first step of **4** differ from those reported earlier,[6a] namely $\Delta H^{\neq} = 62 \pm 3$ kJ mol^{-1} and $\Delta S^{\neq} = -140 \pm 10$ J K^{-1} mol^{-1} at 316 K being in better agreement with the values reported for the reaction of **4** with CN^- ($\Delta H^{\neq} = 76.2 \pm 2.8$ kJ mol^{-1} and $\Delta S^{\neq} = -75.6 \pm 9.2$ J K^{-1} mol^{-1} at 298 K).[6b]

Table 3. Activation parameters for the substitution reactions of the compounds **1**–**6** by thiourea at 298.2 K.[a]

Compound	$\Delta H^{\neq}$ [kJ mol^{-1}]	$\Delta S^{\neq}$ [J K^{-1} mol^{-1}]
	first rate-determining step	
1	86 ± 2 (ado-N7)	−46 ± 5 [−52 ± 5][b] (ado-N7)
2	81 ± 4 (ado-N1)	−77 ± 13 (ado-N1)
	83 ± 4 (ado-N7)	−68 ± 12 (ado-N7)
3	95 ± 3 (ado-N1)	−36 ± 8 [−42 ± 8][b] (ado-N1)
4	90 ± 2 (guo-N7)	−40 ± 7 [−46 ± 7][b] (guo-N7)
5	81 ± 2 (ado-N1)	−80 ± 5 (ado-N1)
	83 ± 2 (guo-N7)	−71 ± 5 (guo-N7)
6	84 ± 3 (guo-N7)	−57 ± 9 (guo-N7)
	81 ± 4 (ado-N7)	−75 ± 13 (ado-N7)
	second rate-determining step	
(guo-N7)	80 ± 1 [from **4**]	−80 ± 7 [from **4**]
	78 ± 3 [from **5**]	−86 ± 9 [from **5**]
	78 ± 4 [from **6**]	−82 ± 12 [from **6**]
(ado-N1)	83 ± 1 [from **3**]	−64 ± 1 [from **3**]
	83 ± 1 [from **2**]	−63 ± 2 [from **2**]
	81 ± 3 [from **5**]	−71 ± 10 [from **5**]
(ado-N7)	82 ± 3 [from **1**]	−64 ± 9 [from **1**]
	84 ± 3 [from **2**]	−58 ± 8 [from **2**]
	82 ± 5 [from **6**]	−63 ± 16 [from **6**]

[a] The bond cleaved in parentheses. [b] Statistically corrected value (k_1/2).

Roughly speaking, the ability of thiourea to displace nucleosides from various bis-complexes follows the thermodynamic stability of different binding modes, that is, guo-N7 > ado-N1 > ado-N7.[16] However, there are a few significant exceptions. In particular, the differences in lability between **4** and **6** are of interest, since these species represent models for the two most abundant Cisplatin–DNA adducts. In the first rate-determining step the reactivity of the mixed-ligand complex **6** is about twice as high as that of the bis(guanosine) complex. Most surprisingly, it is the guo-N7 bond in **6** that is more efficiently cleaved by thiourea (about twice as fast as one of the guo-N7 bonds in **4**). This is in contrast to the behaviour of the ado-N7 bond, the cleavage of which in **6** (and **2**) is slower (ca. 50%) than in symmetric species **1**. It is noteworthy that the cleavage of the guo-N7 bond in **5** is comparable to that of **4** (statistically corrected).

In all cases the *trans*-effect of the NH_3 group on the nucleosides is expected to remain the same. Hence, the differences in the substitution rate constants may be attributed to the *cis*-effect of the neighbouring group and/or to the ability of the complexes to form alternative five-coordinate intermediates upon attack of thiourea. In the first rate-determining step, the latter explanation may be the more relevant because of the similarity of the complexes. Thus, with asymmetric complexes **2**, **5** and **6**, two different five-coordinate species denoted as **IM1** and **IM2** may be formed upon thiourea attack (Scheme 4). Although an unequal contribution of the proposed pathways explains the behaviour of asymmetric complexes, factors accounting for the preponderant dissociation of guo-N7 in **6** remain unclear. It is important to note, however, that in the present case the formation of two different intermediates, **IM1** and **IM2**, does not necessarily require the unusual pseudorotation mechanism suggested very recently for the substitution of [Pt(dien)(L-N7)]$^{2+}$ (L = ado or guo) by thiourea in acidic aqueous solution.[16]

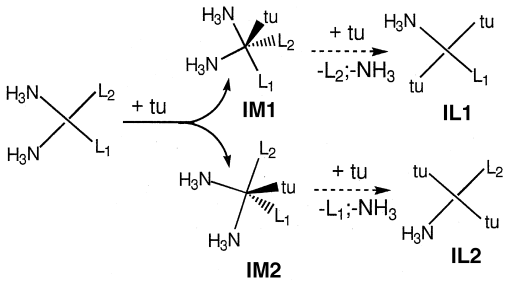

Scheme 4. The two different five-coordinate species possibly formed by asymmetric complexes upon thiourea attack.

Conclusion

In aqueous solution *cis*-[Pt(NH$_3$)$_2$(H$_2$O)$_2$]$^{2+}$ forms different bis(nucleoside) complexes with an excess of either adenosine or a mixture of adenosine and guanosine. Treatment of the reaction mixtures at elevated temperature results in a slow N7 → N1 linkage isomerisation in the adenine moiety only. Most probably the isomerisation involves the breaking and reformation of Pt–nucleoside bonds, thus favouring the thermodynamically more stable N1 binding mode of the adenine base. The dynamic processes due to the presence of adenosine in the platinum coordination sphere are slow on the NMR time scale. These are presumably a result of slow

0947-6539/00/0618-3410 $ 17.50+.50/0 *Chem. Eur. J.* **2000**, *6*, No. 18

rotation about the Pt–nucleoside bond(s); they are most prominent in the ado-N1 binding mode, in line with earlier findings.[17, 19] The N7 binding mode of Pt^{II} in *cis*-$[Pt(NH_3)_2(ado\text{-}N7)_2](ClO_4)_2 \cdot 3.5\,H_2O$ was confirmed by X-ray crystal structure analysis. In both crystallographically independent cations, the Pt^{II} coordination sphere is almost square planar, with normal Pt–N bond lengths and angles. The most significant difference between the two cations can be seen in the sugar conformation. In one cation, both coordinated nucleosides have an *anti* ($-ap$) conformation, whilst in the other cation one nucleoside has an *anti* ($-ap$) conformation and the other a *syn* ($+sc$) conformation stabilised by a relatively strong H-bond O(5′b)···N(3b) of 2.74(2) Å. Substitution of the nucleoside(s) by thiourea follows an associative mechanism with only a negligible contribution from the solvent path. With symmetric complexes, the lability for different binding modes is ado-N1 < guo-N7 < ado-N7 upon substitution of the first nucleoside, whereas the lability of the second nucleoside increases in the order guo-N7 < ado-N1 < ado-N7. In the case of the asymmetric complexes, two parallel reaction pathways explain the concomitant cleavage of different Pt^{II}–nucleoside bonds. The change in the Pt^{II} coordination sphere affects the lability of the coordinating nucleosides in a different manner. The presence of the ado-N1 binding mode renders all binding modes less labile, whereas the ado-N7 mode has the opposite effect. The guo-N7 mode has both influences; it increases the lability of the ado-N1 mode and decreases that of the ado-N7 mode. The differences in lability are very interesting, particularly between **4** and **6** which are considered models for the two most abundant Cisplatin–DNA adducts. The mixed-ligand complex **6** is far more susceptible to attack by thiourea (and perhaps also other nucleophiles) than the symmetric species **4**. This is a result of the increased lability of the guo-N7 mode in the presence of the ado-N7 mode upon dissociation of the first nucleoside, which yields species inherently more labile because of the ado-N7 binding mode. Thus, the enhanced lability of the mixed-ligand complex in the presence of sulfur-containing nucleophiles may explain, at least partly, the preponderance of guo-N7 bisadduct in Cisplatin-treated DNA.

Experimental Section

Materials: The nucleobase derivatives were commercial products from Sigma, and were used as received.[33] Thiourea (99 + %, Aldrich) was recrystallised from methanol. $[Pt(tu)_4]Cl_2$ was synthesised by a literature method.[34] All other chemicals were of the highest purity available and were used as received. A *cis*-$[Pt(NH_3)_2(H_2O)_2]^{2+}$ solution was obtained by treating the corresponding diiodo compound with $AgNO_3$, as previously described.[17]

For the preparation of ***cis*-$[Pt(NH_3)_2(ado\text{-}N7)_2]^{2+}$ (1)**, adenosine (320 mg, 1.2 mmol) was dissolved in 1.5 mL of 1M $HClO_4$ (strongly acidic conditions are required to prevent N(1) platination) followed by the addition of 0.5 equiv of *cis*-$[Pt(NH_3)_2(H_2O)_2]^{2+}$ in 5 mL of water. After being stirred for 3 d at ambient temperature, the mixture was neutralised (pH 7.2) with 1M NaOH, filtered and then concentrated to ca. 1.5 mL. Slow cooling at +4 °C afforded 220 mg (28% from Pt) of *cis*-$[Pt(NH_3)_2(ado\text{-}N7)_2](ClO_4)_2 \cdot 3.5\,H_2O$ (**1a**) as thick, colourless plates. $C_{20}H_{39}Cl_2N_{12}O_{19.5}Pt$ (1025.62): calcd C 23.42, H 3.83, N 16.39; found C 23.22, H 3.69, N 16.04.

Solutions of the other bis(adenosine) complexes, viz., ***cis*-$[Pt(NH_3)_2(ado\text{-}N1)(ado\text{-}N7)]^{2+}$ (2)** and ***cis*-$[Pt(NH_3)_2(ado\text{-}N1)_2]^{2+}$ (3)**, were obtained by treating the mixture of adenosine (320 mg, 1.2 mmol) and *cis*-$[Pt(NH_3)_2(H_2O)_2]^{2+}$ (0.5 equiv) in 10 mL of water for 10 d at 60–70 °C (excess of adenosine was used to prevent unwanted side reactions[19]). After concentration to ca. 2 mL, the mixture was fractionated on a preparative RP-18 column (30 × 200 mm, 40 μm) with 0.1M $NaClO_4$ and 1mM $HClO_4$ in 10% methanol as eluent. Excess electrolyte from the combined fractions of **2** and **3** was removed by refractionating with 10% methanol in 1mM $HClO_4$ to give stock solutions of isomerically pure **2** and **3**, as deduced by HPLC analysis.[35]

Solutions of the complexes ***cis*-$[Pt(NH_3)_2(guo\text{-}N7)_2]^{2+}$ (4)**, ***cis*-$[Pt(NH_3)_2(ado\text{-}N1)(guo\text{-}N7)]^{2+}$ (5)** and ***cis*-$[Pt(NH_3)_2(ado\text{-}N7)(guo\text{-}N7)]^{2+}$ (6)** were obtained in a similar manner by fractionating the reaction mixture containing guanosine (127 mg, 0.4 mmol), adenosine (187.3 mg, 0.7 mmol) and *cis*-$[Pt(NH_3)_2(H_2O)_2]^{2+}$ (0.44 equiv) in 10 mL of water that was stirred for 10 d at 60–70 °C. The isomeric purity of the different isolated fractions was ascertained by HPLC analysis. For comparison, **4** was also prepared by the reaction[36] of guanosine (80 mg, 0.25 mmol) with *cis*-$[Pt(NH_3)_2(H_2O)_2]^{2+}$ (0.12 equiv) followed by LC purification.

Kinetic measurements: Kinetics for the thiourea-assisted dissociation of Pt^{II}–bis(nucleoside) complexes were studied in aqueous solution at different temperatures and monitored using HPLC. A large excess of thiourea ([tu]:[Pt] > 40:1) was used to create pseudo-first-order conditions. The measurements were carried out in buffered solution at pH 4 (0.05M HAc/NaAc);[37] for comparison a few runs were carried out at pH 3–4, the pH being adjusted with 1.0M $HClO_4$. In each measurement, the pH of the reaction mixture remained practically constant (within 0.2 log units). Peak areas at 260 nm were used as the measure of the concentration by employing 1,3-dimethyluracil as an internal standard. Reactions were started by adding the desired Pt^{II} species to a prethermostatted reaction mixture, the ionic strength of which was adjusted to 0.1M with $NaClO_4$. Samples were withdrawn from the reaction mixture at suitable time intervals and diluted with ice-cold water or 0.01M $HClO_4$ (1:1); they were stored on ice prior to chromatographic analysis.

The observed pseudo-first-order rate constants, $k_{1,obs}$, for the attack of the nucleophiles on **1**–**6** were calculated from the disappearance of the starting material by Equation (3). Here the symbol M represents the *cis*-$Pt^{II}(NH_3)_2$ entity. The term $[\mathbf{ML_2}]_0$ is the initial concentration of the complex and $[\mathbf{ML_2}]_t$ is the concentration at time t.

$$\ln[\mathbf{ML_2}]_t = -k_{1,obs} + \ln[\mathbf{ML_2}]_0 \quad (3)$$

The time-dependent concentration of the first HPLC-detectable reaction product $[\mathbf{IL}]_t$ yields the rate parameters $k_{2,obs}$ by Equation (4) with the $k_{1,obs}$ values from Equation (3). The term $[\mathbf{IL}]_{max}$ is the concentration of this species at the moment t [in Equations (3) and (4) charges are omitted for clarity). For asymmetric complexes **2**, **5** and **6**, the terms $[\mathbf{IL}]_t$, $[\mathbf{IL}]_{max}$ and $k_{2,obs}$ in Equation (4) are replaced by $[\mathbf{IL\,1}]_t$, $[\mathbf{IL\,1}]_{max}$ and $k_{21,obs}$ for the intermediate **IL 1**, and $[\mathbf{IL\,2}]_t$, $[\mathbf{IL\,2}]_{max}$ and $k_{22,obs}$ for the intermediate **IL 2**.

$$\frac{[\mathbf{IL}]_t}{[\mathbf{IL}]_{max}} = \frac{e^{-k_{1,obs}t} - e^{-k_{2,obs}t}}{e^{-k_{1,obs}t_{max}} - e^{-k_{2,obs}t_{max}}} \quad (4)$$

NMR studies: NMR spectra were recorded on a JEOL Alpha 500 spectrometer equipped with either a 5 mm normal-configuration tuneable probe or a 5 mm inverse z axis field-gradient probe operating at 500.16 MHz for ^1H, 125.78 MHz for ^{13}C and 107.21 MHz for ^{195}Pt. The spectra were recorded at 25 °C in D_2O (^1H) or in H_2O/D_2O (^{13}C and ^{195}Pt); the desired amount of the purified fraction was first neutralised and then evaporated to dryness, and the residue dissolved in 600 μL of H_2O/D_2O, followed by reevaporation and dissolution in complete D_2O. The ^1H and ^{13}C spectra were referenced internally to sodium 4,4-dimethyl-4-silapentanesulfonate (DSS), assigned as $\delta = 0.015$ for proton and 0 for carbon; the ^{195}Pt spectra were referenced externally to $[PtCl_4]^{2-}$ ($\delta_{Pt} = -1625$ from $[PtCl_6]^{2-}$). The ^1H and ^{13}C assignments were based on a conventional and concerted application of DEPT, COSY, C–H correlation (CHDEC or HSQC/HMQC) and HMBC experiments and by comparison with the isomeric bis(9-methyladenine) complexes[17] of *cis*-$Pt^{II}(NH_3)_2$ and the Pt^{II}(dien) complexes of adenosine.[19] Exchanging spins were also assigned by 2D EXSY experiments. Further experimental details can be found in the Supporting Information. The ^1H chemical shifts in the aromatic region for **1**–**6** are listed in Table 1 and the complete spectral data are given in Table S1 for the ^1H chemical shifts and in Table S2 for the ^{13}C and ^{195}Pt chemical shifts (Supporting Information).

X-ray crystallography: The X-ray data were collected on a Rigaku AFC5S diffractometer at ambient temperature with $Mo_{K\alpha}$ radiation ($\lambda = 0.71069$ Å). Unit cell parameters were obtained from a least-squares fit of 25 reflections [$41.82 < 2\theta < 44.89°$]. Intensity data were collected by the $\omega/2\theta$ scan technique to a maximum 2θ value of 50°. The intensities of three standard reflections were measured every 150 data points; no intensity decay was apparent. The intensities of the reflections were corrected for Lorenz, polarisation and absorption (empirical) effects.[38] The structures were solved by standard Patterson and difference Fourier methods and refined by full-matrix least-squares calculations employing SHELXL-97.[39] All atoms except hydrogen, water oxygens and disordered O and C atoms were refined with anisotropic temperature factors. The hydrogen atoms located on carbon and nitrogen atoms are at calculated positions. The final cycle of refinement gave for the structure **1a** $R1 = 0.0420$ and $wR2 = 0.0897$ for the observed data [$I > 2\sigma(I)$] and 950 parameters, and $R1 = 0.0712$ and $wR2 = 0.988$ for all data. Crystallographic data and experimental details are given in Table 4; selected bond lengths and angles are given in Figure 3 for one of the independent cations of **1a**. Data reduction and subsequent calculations were performed with teXsan for Windows.[40] Figures were drawn with ORTEP-3 for Windows.[41] Crystallographic data (excluding structure factors) for the structure reported in this paper have been deposited with the Cambridge Crystallographic Data Centre as supplementary publication no. CCDC-138213. Copies of the data can be obtained free of charge on application to CCDC, 12 Union Road, Cambridge, CB2 1EZ, UK (fax: (+44) 1223 336-033; e-mail: deposit@ccdc.cam.ac.uk).

Acknowledgements

Financial support from the University Foundation of Turku is gratefully acknowledged. This work is a part of the COST Action D8/004/97 (Chemistry of Metals in Medicine).

Table 4. Crystal structure data and data collection parameters for *cis*-$[Pt(NH_3)_2(adenosine\text{-}N7)_2](ClO_4)_2 \cdot 3.5\,H_2O$ (**1a**).

	1a
formula	$C_{20}H_{39}Cl_2N_{12}O_{19.5}Pt$
M_r	1025.62
system	orthorhombic
space group	$P2_12_12_1$ (no. 19)
a [Å]	19.655(3)
b [Å]	25.122(4)
c [Å]	14.276(6)
α [°]	90
β [°]	90
γ [°]	90
V [Å^3]	7049(3)
Z	8
ρ_{calcd} [Mg m^{-3}]	1.933
absorb. coeff. [mm^{-1}]	4.231
crystal size [mm]	$0.42 \times 0.40 \times 0.38$
no. meas. refl.	6876
no. unique refl.	6825
no. obs. refl.	6825
T_{min}, T_{max}	0.9093, 1.000
variation obs. stand.	− 3.6 %
decay correction	linear
refinement type	on F^2
$R1$ [$I > 2\sigma(I)$][a]	0.0420
$wR2$ [$I > 2\sigma(I)$][b]	0.0897
GoF (= S)[c]	1.025
parameters refined	949
absolute structure parameter	− 0.005(11)
$(\Delta/\rho)_{min}$ [e Å^{-3}]	− 0.689
$(\Delta/\rho)_{max}$ [e Å^{-3}]	1.192

[a] $R1 = \Sigma \,||F_o| - |F_c|| / \Sigma \,|F_o|$. [b] $wR2 = \{\Sigma[w(F_o^2 - F_c^2)^2] / \Sigma[w(F_o^2)^2]\}^{1/2}$ and $w = 1/[\sigma^2(F_o^2) + (aP)^2 + bP)]$, where $P = (2F_c^2 + F_o^2)/3$. [c] $\{\Sigma[w(F_o^2 - F_c^2)^2] / (n-p)\}^{1/2}$, where n = no. of reflections and p = no. of refined parameters.

[1] For a very recent and comprehensive collection of review articles, see: *Cisplatin—Chemistry and Biochemistry of a Leading Anticancer Drug* (Ed.: B. Lippert), Helvetica Chimica Acta, Zürich, **1999**.
[2] a) Z. Guo, P. J. Sadler, *Angew. Chem.* **1999**, *111*, 1610 – 1630; *Angew. Chem. Int. Ed.* **1999**, *38*, 1512 – 1531; b) J. Reedijk, *Chem. Rev.* **1999**, *99*, 2499 – 2510; c) J. Arpalahti in *Perspectives on Bioinorganic Chemistry, Vol. 4*. (Eds.: R. W. Hay, J. R. Dilworth, K. B. Nolan), JAI, Stamford, Connecticut, **1999**, pp. 165 – 208.
[3] a) N. Farrell, *Met. Ions Biol. Syst.* **1996**, *32*, 603 – 639; b) M. Coluccia, A. Nassi, F. Loseto, A. Boccarelli, M. A. Mariggio, D. Giordano, F. P. Intini, P. Caputo, G. Natile, *J. Med. Chem.* **1993**, *36*, 510 – 512.
[4] B. Lippert, *Coord. Chem. Rev*, **1999**, *182*, 263 – 295.
[5] B. Lippert, *Progr. Inorg. Chem.* **1989**, *37*, 1 – 97.
[6] a) J. A. Beaty, M. M. Jones, *Inorg. Chem.* **1992**, *31*, 2547 – 2551; b) M. M. Jones, J. A. Beaty, *Inorg. Chem.* **1991**, *30*, 1584 – 1587.
[7] H. Urata, M. Akagi, *Biochem. Biophys. Res. Commun.* **1989**, 161, 819 – 824.
[8] M. Schmülling, B. Lippert, R. van Eldik, *Inorg. Chem.* **1994**, *33*, 3276 – 3280.
[9] G. Raudaschl-Sieber, B. Lippert, *Inorg. Chem.* **1985**, *24*, 2426 – 2432.
[10] G. Frommer, B. Lippert, *Inorg. Chem.* **1990**, *29*, 3259 – 3260.
[11] M. Boudvillain, R. Dalbiès, M. Leng, *Met. Ions Biol. Syst.* **1996**, *33*, 87 – 103.
[12] D. Yang, S. S. G. E. van Boom, J. Reedijk, J. H. van Boom, A. H.-J. Wang, *Biochemistry* **1995**, *34*, 12912 – 12920.
[13] a) B. Lippert, H. Schöllhorn, U. Thewalt, *J. Am. Chem. Soc.* **1986**, *108*, 6616 – 6621; b) F. Pichierri, D. Holtenrich, E. Zangrando, B. Lippert, L. Randaccio, *J. Biol. Inorg. Chem.* **1996**, *1*, 439 – 445; c) J. Müller, E. Zangrando, N. Pahlke, E. Freisinger, L. Randaccio, B. Lippert, B. *Chem. Eur. J.* **1998**, *4*, 397 – 405.
[14] J. Viljanen, K. D. Klika, R. Sillanpää, J. Arpalahti, *Inorg. Chem.* **1999**, *38*, 4924 – 4925.
[15] a) S. S. G. E. van Boom, J. Reedijk, *J. Chem. Soc. Chem. Commun.* **1993**, 1397 – 1398; b) K. J. Barnham, M. I. Djuran, P. del S. Murdoch, J. D. Ranford, P. J. Sadler, *J. Chem. Soc. Dalton Trans.* **1995**, 3721 – 3725; c) C. D. W. Fröhling, W. S. Sheldrick, *J. Chem. Soc. Chem. Commun.* **1997**, 1737 – 1738.
[16] M. Mikola, K. D. Klika, A. Hakala, J. Arpalahti, *Inorg. Chem.* **1999**, *38*, 571 – 578.
[17] J. Arpalahti, K. D. Klika, S. Molander, *Eur. J. Inorg. Chem.* **2000**, 1007 – 1013.
[18] An endcapped RP-18 column (250×4 mm, 5 μm, E. Merck), water/methanol (88/12) mixture (pH 3, 0.05 M $NaClO_4$) as an eluent, flow rate 1.0 mL min^{-1}.
[19] J. Arpalahti, K. D. Klika, R. Sillanpää, R. Kivekäs, *J. Chem. Soc. Dalton Trans.* **1998**, 3594 – 3598.
[20] J. Arpalahti, K. D. Klika, *Eur. J. Inorg. Chem.* **1999**, 1199 – 1201.
[21] J. Arpalahti, B. Lippert, *Inorg. Chem.* **1990**, *29*, 104 – 110.
[22] M. Ritala, J. Arpalahti, *Inorg. Chem.* **1991**, *30*, 2826 – 2828.
[23] T. G. Appleton, J. R. Hall, S. F. Ralph, *Inorg. Chem.* **1985**, *24*, 4685 – 4693.
[24] M. Polak, J. Plavec, A. Trifonova, A. Földesi, J. Chattopadhyaya, *J. Chem. Soc. Perkin Trans. 1*, **1999**, 2835 – 2843.
[25] A. P. G. Beevers, E. M. Witch, B. C. N. M. Jones, R. Cosstick, J. R. P. Arnold, J. Fisher, *Magn. Reson. Chem.* **1999**, *37*, 814 – 820.
[26] L. Grøndahl, J. Josephsen, R. M. Bruun, S. Larsen, *Acta Chem. Scand.* **1999**, *53*, 1069 – 1077.
[27] W. Saenger, *Principles of Nucleic Acid Structure*, Springer, New York, **1984**, chapter 4.
[28] A half-life of about 23 years has been estimated for the direct NH_3 exchange in $[Pt(NH_3)_4]^{2+}$ at 25 °C in aqueous NH_3 solution; see: B. Brønnum, H. S. Johansen, L. H. Skibsted, *Inorg. Chem.* **1992**, *31*, 3023 – 3025.
[29] Although two intermediates were detected for **6**, they could not be satisfactorily resolved for quantitative analysis.
[30] The fitting procedure in Microcal Origin, version 3.5, Microcal Software, Northampton, MA 01060 (USA), **1994**.
[31] J. Arpalahti, P. Lehikoinen, *Inorg. Chim. Acta* **1989**, *159*, 115 – 120.
[32] J. Arpalahti, P. Lehikoinen, *Inorg. Chem.* **1990**, *29*, 2564 – 2567.
[33] Guanosine contained 1.75 mol of crystal water (TG analysis).
[34] J. Arpalahti, B. Lippert, H. Schöllhorn, U. Thewalt, *Inorg. Chim. Acta* **1988**, *153*, 51 – 55.

  0947-6539/00/0618-3412 $ 17.50+.50/0

[35] It appears that **2** easily decomposes when pH < 3, yielding unidentified products.
[36] 24 h at ambient temperature.
[37] M. Mikola, J. Arpalahti, *Inorg. Chem*. **1996**, *35*, 7556 – 7562.
[38] A. C. T. North, D. C. Phillips, F. S. Mathews, *Acta Crystallogr*. **1968**, *A24* 351 – 359.
[39] G. M. Sheldrick, SHELXL 97, *Program for the Refinement of Crystal Structures*, University of Göttingen, **1997**.
[40] teXsan for Windows, *Structure Analysis Software*, Molecular Structure Corporation, TX 77381 (USA), **1997**.
[41] L. J. Farrugia, *J. App. Cryst.* **1997**, *30*, 565.

Received: January 19, 2000 [F2245]